Bioconjugate Chemistry

Article

pubs.acs.org/bc

Ferritin Decorated PLGA/Paclitaxel Loaded Nanoparticles Endowed with an Enhanced Toxicity Toward MCF-7 Breast Tumor Cells

Ludmila N. Turino,[§] Maria R. Ruggiero,[†,‡] Rachele Stefanìa,[†] Juan C. Cutrin,[†] Silvio Aime,[†] and Simonetta Geninatti Crich*[,†]

[§]Laboratorio de Química Fina, Instituto de Desarrollo Tecnológico para la Industria Química (INTEC), Universidad Nacional del Litoral, Consejo Nacional de Investigaciones Científicas y Técnicas (CONICET), Predio CCT-CONICET, Ruta Nacional 168 Km. 0, 3000 Santa Fe, Argentina

[†]University of Turin, Department of Molecular Biotechnology and Health Sciences, via Nizza 52, 10126, Turin, Italy

[‡]SAET S.p.A, via Torino 213, 10040 Leinì, Turin, Italy

S *Supporting Information*

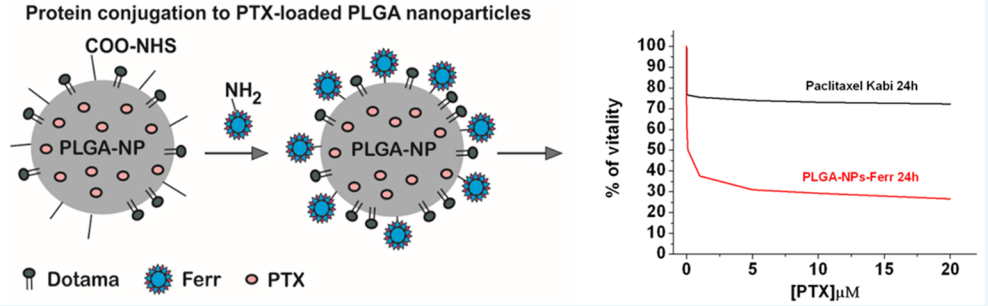

ABSTRACT: Polylactic and glycolic acid nanoparticles (PLGA-NPs), coated with L-ferritin, are exploited for the simultaneous delivery of paclitaxel and an amphiphilic Gd based MRI contrast agent into breast cancer cells (MCF7). L-ferritin has been covalently conjugated to the external surface of PLGA-NPs exploiting NHS activated carboxylic groups. The results confirmed that nanoparticles decorated with L-ferritin have many advantages with respect to both albumin-decorated and nondecorated particles. Ferritin moieties endow PLGA-NPs with targeting capability, exploiting SCARA5 receptors overexpressed by these tumor cells, that results in an increased paclitaxel cytotoxicity. Moreover, protein coating increased nanoparticle stability, thus reducing the fast and aspecific drug release before reaching the target. The theranostic potential of the nanoparticles has been demonstrated by evaluating the signal intensity enhancement on T_1-weighted MRI images of labeled MCF7 cells. The results were compared with that obtained with MDA cells used as negative control due to their lower SCARA5 expression.

INTRODUCTION

Nanotechnology is under intense scrutiny in the design of new medical protocols; a significant improvement of diagnosis and therapy,[1] in particular, of cancer and cardiovascular diseases, is expected from the application of nanosized drug delivery systems.[2] In this context, liposomes, solid-lipid nanoparticles, and biodegradable polymeric nanoparticles are the most widely investigated systems. Poly(D,L-lactide-*co*-glicolide) (PLGA) has attracted great attention in the design of nanosized delivery systems because of its excellent biocompatibility and biodegradability, associated with the presence of ester linkages that undergo slow hydrolysis in aqueous systems.[3] The removal of nanosized drug carriers from the body, due to their hydrophobic nature, by the Mononuclear Phagocyte System is a major obstacle that hinders the application of these drug delivery systems.[4] Therefore, surface modification and coating of PLGA nanoparticles is the subject of studies aimed at prolonging their circulation lifetime. The most commonly used strategy to obtain stealth nanoparticles is based on the use of PEG and it has led to the development of several products that are currently in clinical use.[5] However, the recent observation of anti-PEG immunological response[6] has motivated renewed interest toward the research for alternative strategies. Among possible surface modification of PLGA nanoparticles, serum albumin has received some attention due to its relatively small size, hydrophilic surface, and accumulation in the leaky vasculature of tumors through passive targeting.[7−9] PLGA nanoparticles coated with serum albumin showed improved stability, and when loaded with the antitumoral paclitaxel drug, more efficient delivery to tumor cells. Herein we report results concerning the use of ferritin as alternative protein coating for PLGA surface. In addition to act as a hydrophilic cover, ferritin may endow the nanoparticle with a potential targeting capability, thus improving the uptake from the tumor cells through specific ferritin receptors. Ferritin is the main iron

Received: February 20, 2017
Published: March 16, 2017

DOI: 10.1021/acs.bioconjchem.7b00096
Bioconjugate Chem. 2017, 28, 1283−1290

storage protein and is composed of 24 subunits of heavy (H)- or light (L)-chain polypeptides that are present at different ratios in various organs to form a cage architecture of 12 nm in external diameter, with an inner cavity of 8 nm.[10] Ferritin functions are traditionally associated with intracellular iron storage, but additional functions related to iron delivery based on a transferrin-independent mechanism to different target organs (such as brain, liver, and spleen) have been recently discovered and investigated.[11] The involved receptors belong to scavenger receptor class A member 5 (SCARA5)[12−14] for L-ferritin and to TIM-2[15] and TfR-1[16,17] for H-ferritin, in mice and human, respectively. Based on evidence attained from both epidemiological and molecular studies, new insights link the presence of excess iron and altered iron metabolism to cancer as a consequence of the rapid cell proliferation.[18] It is well-known that many cancer cells reprogram iron metabolism in ways that result in net iron influx.[19] This occurs through the up-regulation of the expression of proteins that are involved in iron uptake (i.e., TfR1, SCARA5) and the decreased expression of iron efflux proteins, such as ferroportin. The relationship between ferritin and cancer is well supported by studies showing an increase of the total ferritin (rich in L-chains) in the blood serum.[20] For example, in breast cancer patients, a correlation was found with ferritin increase and the stage of the disease, as the high serum concentration of the protein is associated with the release within the breast tumor micro-environment.[21] Accordingly, breast tumor lysates also show elevated levels of L-ferritin, the predominant subunit observed in serum, and this increase correlates with advanced histological grade and poor outcome.[22,23] There are many examples in the literature exploiting ferritin for the delivery of water-soluble drugs and imaging agents loaded in its inner aqueous cavity.[24−27] In this context, we have previously reported that native horse spleen ferritin (composed of 85% and 15% L and H chains, respectively) is selectively taken up by the human breast cancer cell line MCF7 through SCARA5 receptors.[28]

On this basis, herein we propose the use of ferritin as simultaneous targeting and coating agent for PLGA nanoparticles, able to selectively deliver paclitaxel (PTX), a cytostatic compound with very low water solubility, to breast cancer (MCF-7 cells). Horse spleen ferritin has been covalently conjugated to the external surface of PLGA nanoparticles exploiting NHS activated carboxylic groups (Figure 1A). Moreover, PLGA nanoparticles have been loaded with a Gd based MRI imaging agent (Gd-DOTAMA, Figure 1B), in order to monitor their distribution. The performance of ferritin functionalized PLGA nanoparticles has been compared with the corresponding albumin coated ones as well as with unfunctionalized particles.

RESULTS AND DISCUSSION

Preparation of PLGA Nanoparticles (PLGA-NPs). PLGA is one of the most attractive biodegradable and biocompatible polymers that has been used in a number of applications, ranging from drug delivery to tissue engineering.[29] PLGA nanoparticles are characterized by a hydrophobic core that enables entrapping water insoluble hydrophobic molecules. PLGA-NPs were obtained by the o/w emulsion solvent extraction method. The organic phase was prepared by dissolving PLGA or PLGA-NHS and Gd-DOTAMA complex in chloroform.[30] The water phase was a poly(vinyl alcohol) (PVA) aqueous solution. PVA is the most commonly used emulsifier for the preparation of PLGA-based NPs because it

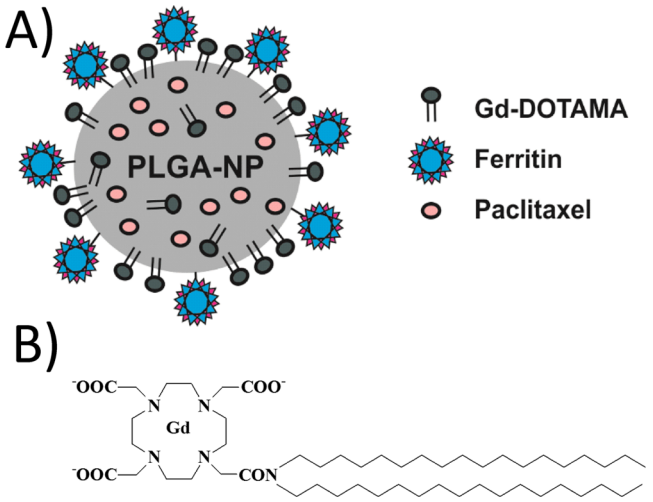

Figure 1. (A) Schematic representation of PLGA-Ferr nanoparticles. (B) Schematic representation of Gd-DOTAMA.

yields particles that are relatively uniform, small sized, and easy to redisperse in water.[31] The organic phase was added to the aqueous phase, and then the resulting mixture was extensively sonicated. The nanoparticles were obtained by the slow organic solvent evaporation of the o/w emulsion. Then, ferritin (Horse Spleen Ferritin) or bovine serum albumin (BSA) was covalently conjugated to PLGA-NHS nanoparticles exploiting the reaction of PLGA−NHS with the amine groups present on the protein external surface.[32−34] Before conjugation, ferritin was purified by gel filtration chromatography to eliminate high-molecular-weight aggregates whereas BSA was used without further purification. The reaction was carried out overnight, at room temperature, under magnetic stirring. Pure PLGA-Ferr and PLGA-BSA have been obtained after size exclusion chromatography (see Supporting Information, Figure S1). Control nanoparticles (PLGA-CTRL), without protein coating, were synthesized following the same synthetic protocol using the commercially available PLGA with unconjugated carboxylic groups. As reported in Table 1 both the average PLGA hydrodynamic diameters (measured by dynamic light scattering) and the longitudinal relaxation rate of water protons ($1/T_1$) of the conjugated nanoparticles were unaffected by the protein conjugation. The amount of Ferritin or BSA bound to

Table 1. Hydrodynamic Particle Diameter Measured by DLS at 25 °C in HBS Buffer and Polydispersity Index (PDI) of PLGA-CTRL, PLGA-Ferr, and PLGA-BSA Are Reported Together with Their Millimolar Relaxivities (mM^{-1} s^{-1}) and of Gd-DOTAMA and Protein Encapsulation Yields[a]

	PLGA-CTRL	PLGA-Ferr	PLGA-BSA
size (nm)	152 ± 8	157 ± 9	154 ± 14
PDI	0.193 ± 0.024	0.214 ± 0.043	0.141 ± 0.007
r_{1p} (mM^{-1} s^{-1})	26.6 ± 1	29.3 ± 0.93	29.7 ± 0.3
Gd-DOTAMA (%)	57 ± 14	38 ± 10	39 ± 11
protein (%)		3.7 ± 0.8	4.7 ± 0.7
number of proteins/NP		121 ± 25	763 ± 83
number of Gd/NP	$1.0 \times 10^5 \pm 0.1 \times 10^5$	$1.3 \times 10^5 \pm 0.3 \times 10^5$	$1.0 \times 10^5 \pm 0.15 \times 10^5$

[a]The table shows the mean ± SEM of 5 independent experiments.

DOI: 10.1021/acs.bioconjchem.7b00096
Bioconjugate Chem. 2017, 28, 1283−1290

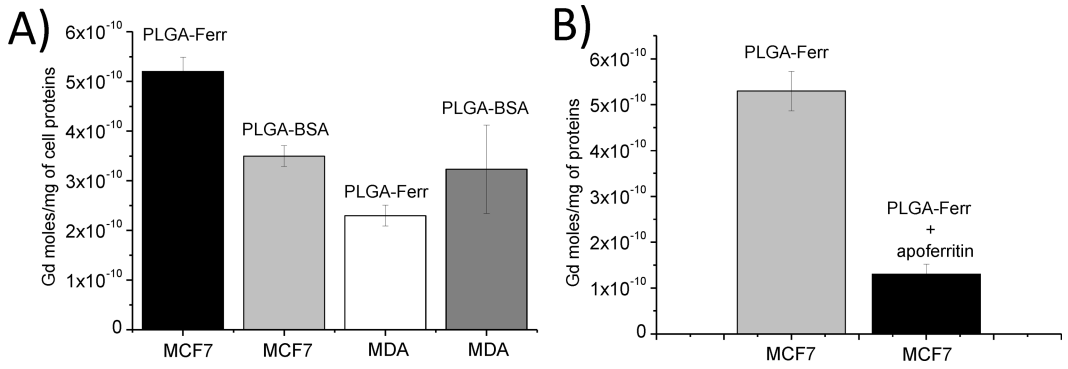

Figure 2. (A) ICP-MS determination of the intracellular Gd content of MCF7 and MDA-MB-231 cells cultured for 6 h with PLGA-Ferr and PLGA-BSA 50 μM in Gd. (B) Competition experiment on MCF7 cells. ICP-MS measurements of intracellular Gd were done with or without the addition of an excess (75-fold) of native ferritin. Graphs show the mean ± SEM of internalized Gd mol per mg of total cell proteins from 3 independent experiments.

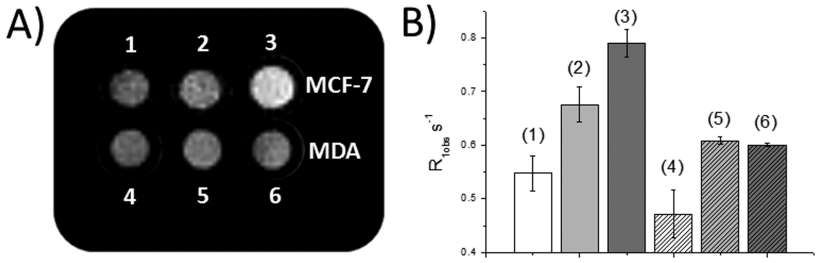

Figure 3. (A) Representative T_1-weighted spin−echo image (acquired at 7T) of glass capillaries containing MCF7 (1, 2, 3) and MDA-MB-231 (4, 5, 6) cells incubated for 6 h in the absence (1, 4 controls) and in the presence of PLGA-BSA (2, 5) and PLGA-Ferr (3, 6). (B) R_{1obs} (s^{-1}) measured on cell pellets using a saturation recovery sequence. The histogram shows the mean ± SD of R_{1obs} from 3 independent experiments.

PLGA-NPs after size exclusion chromatography purification was 0.23 ± 0.04 and 0.21 ± 0.03 mg/mL, respectively, which represent approximately 121 ± 25 ferritin and 763 ± 83 BSA molecules per NP, respectively. Interestingly, one may observe that the ratio between the amount of ferritin and BSA bound to PLGA-NPs corresponds approximately to the ratio of the molecular weights of the two proteins. In order to rule out the occurrence of a noncovalent adsorption of the proteins on the PLGA surface, as reported in the literature for serum proteins,[35,36] nonactivated PLGA-CTRL was incubated overnight in the presence of the same amount of ferritin and BSA. The obtained solutions were purified by gel filtration using the same protocol. In the solutions of purified nanoparticles the protein concentrations were in both cases under the detection limit (0.034 mg/mL). The low absorption is the consequence of the lower albumin (BSA) concentration incubated (2 mg/mL) and the negative Z-potential of PLGA-CTRL (−3.9 ± 1.5). The number of GdDOTAMA loaded in one nanoparticle (ca. 1×10^5) is of the same order as those reported for liposomes or other nanoparticles embedded with contrast agents in their interior and not only on their surface.[37,38]

Cellular Uptake of PLGA-Ferr and PLGA-BSA by Human Breast Cancer Cell Lines. The uptake of PLGA-Ferr and PLGA-BSA was assessed in human breast cancer cells MCF-7 and MDA-MB-231, respectively. As already well established,[28] MCF7 expresses a relatively high concentration of SCARA5 receptors on their cytoplasmatic membrane, able to internalize L-ferritin, whereas MDA-MB-231 has been used as a negative control.[28] Cells were incubated in the presence of PLGA-BSA and PLGA-Ferr for 6 h at 37 °C and 5% CO_2. The amount of Gd, as determined by ICP-MS, is taken as a reporter of the extent of cell internalized PLGA nanoparticles. Figure 2A shows the amount of internalized Gd normalized to the total protein cell content. The values of internalized Gd were significantly higher for MCF-7 incubated in the presence of PLGA-Ferr than PLGA-BSA ($p < 0.0241$). On the contrary, Gd uptake into MDA-MB-231 cells was lower and not significantly different for the two types of nanoparticles ($p < 0.249$). This is in agreement with the fact that these cells express lower SCARA5 receptors than MCF-7.[28] Furthermore, the specificity of the uptake was supported by carrying out a competition study in which the MCF7 cells were incubated with PLGA-Ferr for 6 h in the presence of an excess (75-fold) of native ferritin. The Gd uptake, measured by ICP-MS, decreased for about 80% as shown in Figure 2B.

Magnetic Resonance Imaging (MRI). In order to assess whether Gd-labeled PLGA-NPs can generate a sufficient MRI contrast for targeted cells MCF7 and MDA-MB-231, T_1-weighted MR images were acquired on cellular pellets obtained upon incubation with PLGA-Ferr and PLGA-BSA (50 μM of Gd), respectively. Figure 3A shows that MCF-7 incubated with PLGA-Ferr displayed markedly higher signal intensity when compared to untreated cells or treated with PLGA-BSA. Only small changes in signal intensity (SI) were observed in MDA-MB-231 cells incubated in the absence or in the presence of PLGA-Ferr and PLGA-BSA, respectively. The differences among the relaxation rates (s^{-1}) (Figure 3B) measured on the cell pellets reflected the observed difference in PLGA-Ferr uptake by MCF-7 and MDA-MB-231 as expected by their different expression of ferritin receptors.

Loading of Paclitaxel in PLGA-NPs. In order to design a "theranostic" system containing both imaging and therapeutic agents, paclitaxel (PTX) has been added to the previously described PLGA-NPs. Paclitaxel is a drug largely used in the

DOI: 10.1021/acs.bioconjchem.7b00096
Bioconjugate Chem. 2017, 28, 1283−1290

treatment of various types of cancer, including ovarian cancer, breast cancer, nonsmall cell lung cancer, and Kaposi's sarcoma.[39] PTX is characterized by a low solubility in water and it is administered to patients in a micellar formulation based on macrogolglycerol ricinoleate dissolved in ethanol.[40,41] The preparation of PLGA-PTX nanoparticles was performed using the same procedure described above. PTX was dissolved in chloroform together with PLGA or PLGA-NHS and Gd-DOTAMA at an initial PTX amount corresponding to 10% w/w (with respect to PLGA). Then, preformed PLGA nanoparticles were conjugated with the protein (ferritin or BSA). The PTX encapsulation yields, determined by HPLC, were 6.88 ± 0.98, 9.95 ± 1.5, and 27.9 ± 16 (±SEM) for PLGA-PTX-BSA, PLGA-PTX-Ferr, and PLGA-PTX-CTRL, respectively. The significantly lower values found after protein conjugation with respect to the nonfunctionalized PLGA-PTX-CTRL appears to be due to the fact that a non-negligible amount of nanoparticles disappeared during the HPLC purification procedure. In fact, the differences are significantly reduced if the PTX loading efficiency is expressed as Gd/PTX % (21 ± 10, 23 ± 14, 16 ± 3.8 ± SEM for PLGA-PTX-BSA, PLGA-PTX-Ferr, and PLGA-PTX-CTRL, respectively). In vitro drug release from PLGA nanoparticles was evaluated at different intervals of time under dialysis in 1L PBS buffer, as shown in Figure 4. It appears evident that PTX is released more slowly from PLGA-PTX-Ferr and PLGA-PTX-BSA than from PLGA-PTX-CTRL (15 ± 3.4%, 20 ± 4.5%, and 40 ± 2.25% within 6 h, respectively (±SEM).

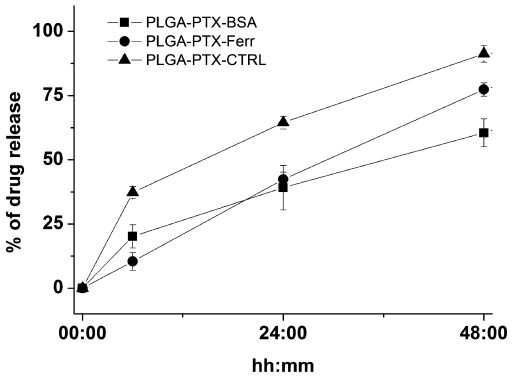

Figure 4. In vitro drug release from PLGA-PTX-CTRL, PLGA-PTX-Ferr, and PLGA-PTX-BSA evaluated at different times (6, 24, 48 h) under dialysis in PBS at 37 °C, pH = 7.4. Graphs show the mean ± SD of % PTX release obtained by 3 independent experiments.

PTX release from nanoparticles depends on drug diffusion at the PLGA surface that, in turn, is affected by "bulk" erosion or swelling.[42] The PTX release behavior from the nanoparticles developed here exhibited a biphasic pattern characterized by an initial rapid release during the first 24 h, followed by a slower and continuous release. The high initial burst release can be attributed to the dissolution of PTX physically adhered at the surface or located at the first layers of the solid nanoparticles.[40] It is likely that the presence of ferritin or BSA on the surface of PLGA-NPs slowed down this burst release compared to PLGA-PTX-CTRL. Furthermore, the presence of protein on the outside layer of NPs could slow down diffusion of hydrophobic PTX to the outside medium, making release slower compared to NP without protein coating. Also, the increasing diffusional distance for PTX molecule may delay the drug release from the core of the NPs.[9,43−45]

Toxicity Test of PLGA-PTX Nanoparticles. Viability assays were performed on MCF-7, as they showed a good capability to take up PLGA-PTX-Ferr nanoparticles. Cells were incubated in the presence of PLGA-PTX-Ferr, PLGA-PTX-BSA, PLGA-PTX-CTRL, and a commercially available Paclitaxel formulation administered to human patients (Paclitaxel Kabi) at increasing concentrations for 6 and 24 h (Figure 5A,B). The range of concentrations of PTX corresponds to plasma levels of the drug achievable in humans.[46] As mentioned above, Paclitaxel Kabi is a water-soluble paclitaxel formulation containing macroglycol ricinolate. In agreement with that previously reported by Esfandyari-Manesh and co-workers,[7] we found that the toxicity, herein evaluated by MTT assay, of PLGA coated with BSA and loaded with PTX (PLGA-PTX-BSA) is significantly higher than that observed for the commercially available Paclitaxel Kabi and for the PTX loaded PLGA-PTX-CTRL. The observed behavior may account for the presence of gp60 (albondin) receptor and caveolar transport, as both systems are involved in the trans-endothelial cell transport of albumin.[7] The data reported in Figure 5 show that the cytotoxicity is further enhanced by using PLGA coated with ferritin that targets tumor cells more efficiently via the up-regulation of SCARA5 receptors. The percent viability of MCF-7 incubated for 6 h with PLGA-Ferr, PLGA-BSA, PLGA-CTRL, and Paclitaxel Kabi (all at a final

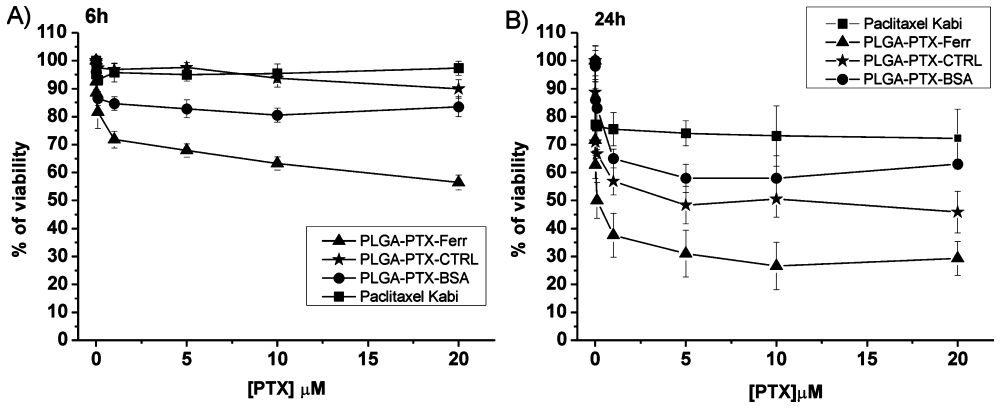

Figure 5. Percentage of viability (measured with MTT assay) of MCF-7 after 6 (A) and 24 h (B) of incubation at different concentrations of PLGA-PTX-CTRL, PLGA-PTX-Ferr, PLGA-PTX-BSA, and Paclitaxel Kabi. Graphs show the mean ± SEM of % viability evaluated on 3 independent experiments.

DOI: 10.1021/acs.bioconjchem.7b00096
Bioconjugate Chem. 2017, 28, 1283−1290

PTX concentration 20 μM) were 56%, 83.5%, 89%, and 97%, respectively (Figure 5).

The low toxicity of the commercial drug is very likely due to the short treatment time, only 6 h, which does not lead to enough internalized drug to have detectable cytotoxic effect. In fact, several experiments are reported in the literature where the therapeutic treatment is continued for more than 24 h.[41] While the percent viability of MCF-7 after 24 h of incubation at 20 μM of PTX with PLGA-PTX-Ferr, PLGA-PTX-CTRL, PLGA-PTX-BSA, and Paclitaxel Kabi were 29%, 45%, 63%, and 72% (Figure 5B). The cytotoxicity of nanoparticles not loaded with paclitaxel was evaluated (see Supporting Information, Figure S4) and it was less than 10% for all the PLGA-NPs after 6 and 24 h incubation. Nanoparticles with or without PTX were incubated with cells at the same Gd concentration. In order to prove the selective toxic effect of PLGA-PTX-Ferr for tumor cells a comparative cytotoxicity study was done on the human mammary nontumorigenic epithelial cell line MCF-10A using the same protocol described above. Figure 6 shows clearly that

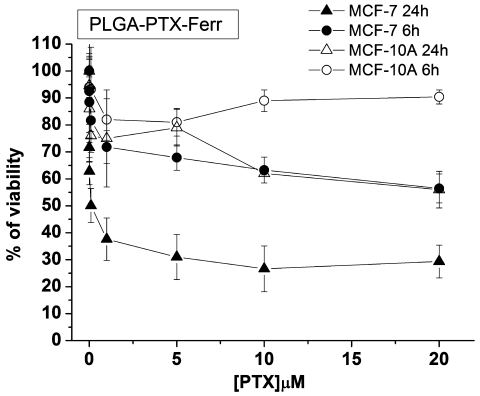

Figure 6. Percentage of viability of MCF-7 and MCF-10A after 6 and 24 h of incubation at different concentrations of PLGA-PTX-Ferr. Graphs show the mean ± SEM of % viability evaluated on 3 independent experiments.

PLGA-PTX-Ferr are significantly more toxic for tumor cells (MCF7) than healthy MCF-10A after 6 and 24 h incubation. From these results one draws the conclusion that the specific uptake of PLGA-PTX-Ferr by breast cancer cells (MCF7) allows an increase in the therapeutic output of PTX thus overcoming some limitation currently encountered in the clinical use of this drug. Indeed, despite the wide spectrum of antitumor activity of PTX, its therapeutic application in cancer therapy is still hampered by its low aqueous solubility (that necessitates the use of Cremophor EL, a noninonic solubilizer and emulsifier where the main component is glycerol polyethylene glycol ricinolate) and poor accumulation at the target tumor cells.[38,39]

CONCLUSIONS

In this work it has been shown that the novel drug delivery system based on hydrophobic PLGA nanoparticles decorated with ferritin has many advantages with respect to nondecorated particles. Ferritin moieties endow the PLGA-NPs with a targeting capability that, in turn, results in an increased cytotoxicity. Although we have considered only the aggressive breast cancer represented by MCF-7 cell line, it is reasonable to expect that similar results could be obtained from any tumor whose cells overexpress ferritin transporters. Moreover, protein coating increases the stability of the nanoparticle thus avoiding the fast and aspecific drug release before reaching the target. Finally, the versatility of the PLGA nanoparticles permits the combination of therapy and diagnosis by entrapping MRI contrast agents inside the PLGA-NPs hydrophobic core, in a single drug delivery system.

EXPERIMENTAL PROCEDURES

Materials. Poly(D,L-lactide-*co*-glicolide) (PLGA) RG 502H 50:50, molecular weight (MW) 30 000−60 000 Da, and poly(vinyl alcohol) (PVA), MW 31 000−50 000 Da (98−99% hydrolyzed), ferritin from equine spleen (Ferr), albumin from bovine serum (BSA), insulin, Thiazoly Blue Tetrazolium Bromide (MTT), *N*-ethyl-*N*′-(3-(dimethylamino)propyl) carbodiimide (EDC), *N*-hydroxysuccinimide (NHS), and acetonitrile were provided by Sigma-Aldrich. Paclitaxel (PTX) was purchased from Aurisco Pharmaceutical Limited (China), while the Paclitaxel Kabi from Fresenius Kabi AG (Italy). The lipophilic Gd-DOTAMA (Figure 1B was synthesized according to a previously reported procedure.[47] Human breast cancer cell lines (MDA-MB-231 and MCF-7) were obtained from ATCC. DMEM and EMEM media, fetal bovine serum (FBS), penicillin, streptomycin, L-glutamine, nonessential amino acid, sodium pyruvate, and MycoAlert PLUS Mycoplasma Detection Kit, were obtained from Lonza (Belgium).

Synthesis of *N*-Hydroxysuccinimide Activated PLGA (PLGA-NHS). PLGA polymer (100 mg, 0.0025 mmol) was dissolved in CH_3CN (1 mL). EDC (20 mg, 0.1 mmol) and NHS (10 mg, 0.09 mmol), both dissolved in CH_3CN (0.5 mL) were subsequently added, to PLGA solution. The reaction was left to stir at room temperature for 12 h. The product was precipitated in diethyl ether and washed several times with diethyl ether/methanol (1:1) and dried under vacuum. The ^{13}C NMR (600 MHz, $CDCl_3$) was used to assess the formation of the NHS ester (Figure S2 in Supporting Information). The disappearance of the carboxyl groups at 174.2 and 171.8 ppm, corresponding to the PLGA carboxylic acid groups, proved the formation of NHS ester.

Preparation of PLGA-NPs. PLGA-NPs were obtained using an oil-in-water (o/w) emulsion solvent extraction method. The emulsion was prepared by dissolving 25 mg of PLGA-NHS, 3.5 mg of Gd-DOTAMA in 0.5 mL of chloroform; this solution was called phase 1. Phase 2 consisted of 3% w/v PVA aqueous solution (3 mL). Phase 1 was added into phase 2 drop by drop and sonicated with a sonicator tip for 300 s at 100% power. Final emulsion was transferred to a 50 mL round-bottomed flask and put into a rotary evaporator at 740 mmHg and 30 rpm for 120 min to remove the organic solvent.

Purification of Ferritin. One milliliter of commercial ferritin was purified to eliminate its high-molecular-weight aggregates by size exclusion chromatography, using an AKTA FPLC Purifier system, equipped with UV−vis detector (set at 215, 280, and 350 nm). Superose 6 10/300 GL was used as column and HBS buffer (1.8 mM Hepes and 150 mM NaCl, pH 7.4) as eluent at a flow rate of 0.5 mL min^{-1}. The fraction which corresponded to ferritin monomer (440 kDa, V_R = 13.2 mL) were collected and concentrated with vivaspin filters (Sartorius) (MWCO 10 000 Da). The final concentration of protein was determined by means of the Bradford assay, using bovine serum albumin as a standard.

Conjugation of Ferritin or Bovine Serum Albumin (BSA) to PLGA-NPs. A solution of BSA or Ferritin in PBS (10 mg/mL) was added to PLGA-NPs solution immediately after

DOI: 10.1021/acs.bioconjchem.7b00096
Bioconjugate Chem. 2017, 28, 1283−1290

nanoparticle preparation using a PLGA/protein ratio of 2.5:1 (25 mg/10 mg). The conjugation reaction between protein and PLGA-NPs was carried out at room temperature overnight under magnetic stirring. The reaction solution was centrifuged at 5000 rpm for 10 min and then purified by size exclusion chromatography using the same purification protocol used for ferritin. Chromatograms before and after purification are reported as Supporting Information (Figure S1). The collected fractions corresponding to conjugated PLGA-NPs (V_R = 6.5 mL) were concentrated with vivaspin filters (Sartorius) (MWCO 10 000 Da) by centrifugation at 5000 rpm. The amount of Gd-DOTAMA entrapped in the PLGA-NPs was determined by using inductively coupled plasma mass spectrometry (ICP-MS; element-2; Thermo-Finnigan, Rodano (MI), Italy). Sample digestion was performed with concentrated HNO_3 (70%, 1 mL) under microwave heating (Milestone MicroSYNTH Microwave Labstation). The hydrated mean diameter of conjugated PLGA-NPs were determined using a dynamic light scattering (DLS) Malvern Zetasizer 3000HS (Malvern, U.K.) All samples were analyzed at 25 °C in filtered (cutoff, 200 nm) NaCl 10 mM buffer (pH 7.4). The relaxivity (r_{1p}) at 21.5 MHz and 25 °C was determined by ^{1}H nuclear magnetic resonance T_1 measurement (Stelar Spinmaster, Mede, Italy) by means of the inversion recovery method (16 delay values, two averages). The reproducibility of the T_1 data was ±5%. The amount of conjugated proteins was determined by means of the Bradford assay, using bovine serum albumin as a standard. The average number of BSA or ferritin molecules conjugated to PLGA-NP was calculated by dividing the number of BSA or ferritin molecules found in the solution (calculated from their final concentration) for the calculated average number (n) of PLGA-NPs. The average number (n) of PLGA-NPs was calculated using the following equation:

$$n = 6m/(\pi \cdot D^3 \cdot \rho) \quad (1)$$

where m is the NP weight, D is the number based on mean NP diameter determined by dynamic light scattering (DLS), and ρ is the NP weight per volume unit (density), estimated to be 1.1 g/cm^3 based on the polymer density.[48] The NP weight (m) was indirectly determined by the GdDOTAMA concentration considering than about 8 mg of GdDOTAMA are loaded into 100 mg of PLGA nanoparticles as estimated by three independent PLGA-NPs preparations, purified by dialysis without centrifugation that causes nanoparticle aggregation and loss.

Cell Lines. MDA-MB-231 cells were cultured in DMEM medium containing 10% (v/v) fetal bovine serum (FBS), 100 U/mL penicillin, 100 U/mL streptomycin, 0.01% and 4 mM L-glutamine. MCF-7 cells were cultured in EMEM medium containing 10% (v/v) FBS, 100 U/mL penicillin and streptomycin, 1% (v/v) nonessential amino acid, 1 mM sodium pyruvate, 2 mM L-glutamine, and 0.01 mg/mL insulin. The MCF 10A cells were cultured in Dulbecco's modified Eagle's medium and Ham's F12 medium supplemented with 20 ng/mL epidermal growth factor, 100 ng/mL cholera toxin, 0.01 mg/mL insulin, 500 ng/mL hydrocortisone, and 5% of horse serum. Cells were incubated at 37 °C under a humidified atmosphere of 5% CO_2. These cell lines were tested for mycoplasma (MycoAlert PLUS Mycoplasma Detection Kit, Lonza).

Uptake Experiments. For PLGA-BSA and PLGA-Ferr uptake experiments, MCF-7 and MDA-MB-231 were seeded at a density of 5 × 10^5 cells in dishes of 6 cm Ø and placed in a wet (37 °C) 5% CO_2 air atmosphere incubator. For the different experiments, at 48 h post seeding, cells were incubated with 50 μM of Gd. After 6 h of incubation, cells were washed three times with 10 mL ice-cold PBS, detached with trypsin/EDTA. The Gd content in each cell line was determined by ICP-MS. For MRI analysis (see below) cells were transferred into glass capillaries. Protein concentration (proportional to the cell number) was determined from cell lysates by the Bradford assay.

MRI. All the MR images were acquired on a Bruker Avance 300 spectrometer (7T) equipped with a Micro 2.5 microimaging probe (Bruker BioSpin, Ettlingen, Germany). Glass capillaries containing about 2 × 10^6 cells were placed in an agar phantom and MR imaging was performed by using a standard T_1-weighted multislice spin−echo sequence (TR/TE/NEX = 250/3.7/8, FOV = 1.2 cm, MTX = 128 × 128, NEX = number of excitations; FOV = field of view). The T_1 relaxation times were calculated using a standard saturation recovery spin echo.

Preparation and Characterization of PTX Loaded PLGA-NPs. Targeted PLGA-NPs loaded with Paclitaxel were obtained using an oil-in-water (o/w) emulsion solvent extraction method. Briefly, 25 mg of PLGA-NHS, 2.5 mg of PTX, and 3.5 mg of Gd-DOTAMA were dissolved in chloroform and the same synthesis procedure described above was followed. Conjugation of ferritin or BSA to PTX loaded PLGA-NPs (PLGA-PTX-NP) was done following the procedure described above. The drug loading efficiency was determined in duplicate by HPLC on Waters Alliance-HPLC system equipped with 2695-separation module connected to 2998-photodiode array. A reverse-phase Waters XBridge C18, 150 mm × 4.6 mm ID, 5 μm at 25 °C was used as the column. The water−acetonitrile was used as the mobile phase in gradient elution mode (acetonitrile: 0−2 min, 40%; 2−10 min, 40−100%). The effluent was monitored at 227 nm and flow rate was 1 mL/min. The retention time (T_r) of PTX was found to be 6.12 min. The PTX stock solution (1 mg/mL), dissolved in acetonitrile, was diluted to the range 10−150 μg/mL for standard calibration curve (R^2 = 0.99984). 30 μL aliquots of PLGA-PTX-NP samples before injection were freeze-dried and then sonicated in an ultrasonic bath in 200 μL chloroform for 30 min. After centrifugation at 5000 rpm for 10 min and evaporation of the chloroform, they were sonicated again with 200 μL acetonitrile for 15 min and then analyzed by HPLC injectin 50 μL of samples. (Supporting Information, Figure S3). The encapsulation efficiency was defined by the ratio of the measured and initial amounts of PTX encapsulated in the nanoparticles.

In Vitro Drug Release. PTX-loaded nanoparticles, dissolved in HBS at a PTX concentration of 57 μg/mL, were transferred to dialysis bags (MWCO 10 000 Da) and placed in 1 L of HBS with stirring at 110 rpm and 37 °C. At determined time intervals (6, 24, and 48 h), 30 μL of PLGA-PTX-Ferr and PLGA-PTX-BSA were taken and freeze-dried. Then the obtained powder was dissolved in 200 μL of chloroform by sonicating in an ultrasonic bath for 30 min. After centrifugation at 5000 rpm for 10 min and chloroform evaporation, the obtained powders were dissolved in 200 μL of acetonitrile, sonicated in an ultrasonic bath for 15 min, and then analyzed by HPLC, as described above.

In Vitro Cellular Viability. MTT test (Sigma-Aldrich) was used to evaluate the in vitro cytotoxicity of PLGA-PTX-Ferr and PLGA -PTX-BSA on MCF-7. MCF-7 cells were seeded at density of 1 × 10^4 viable cells/well in 96-well plates 48 h before

DOI: 10.1021/acs.bioconjchem.7b00096
Bioconjugate Chem. 2017, 28, 1283−1290

experiments. Cells were incubated for 6 h at increasing concentrations of nanoparticles ranging from 0 to 20 μM PTX concentration. After a washing step with 100 μL phosphate buffer, 10 μL of MTT (5 mg/mL in phosphate buffered saline (PBS): NaCl 0.136 M, KCl 2.7 mM, K_2HPO4 8.6 mM, and KH_2PO_4 1.5 mM) was added at 100 μL of medium. After 4 h of incubation, the culture medium containing MTT solution was eliminated and crystals of formazan were dissolved in 150 μL of dimethyl sulfoxide (DMSO). Then, a microplate reader (iMark, BioRad) was used to read it at 570 nm wavelength. The effect of treatment was calculated as a percentage of viability against the controls.

Statistical Analysis. Data were expressed as means ± SEM (standard error of the mean) or ± SD (standard deviation of the mean), as indicated in the different determinations, calculated from at least 3 independent experiments. Statistical analyses were performed using the Student two-tailed *t* test. A *p* value less than 0.05 was considered statistically significant.

■ ASSOCIATED CONTENT

Supporting Information

The Supporting Information is available free of charge on the ACS Publications website at DOI: 10.1021/acs.bioconjchem.7b00096.

Size exclusion chromatography of PLGA nanoparticles; ^{13}C NMR spectra of PLGA and PLGA-NHS (carbonylic region); HPLC chromatograms of paclitaxel loaded into nanoparticles; MTT assay of MCF-7 incubated with PLGA nanoparticles not loaded with paclitaxel (PDF)

■ AUTHOR INFORMATION

Corresponding Author

*E-mail: simonetta.geninatti@unito.it. Tel +39 011 6706473. FAX +39 011 6706487.

ORCID

Simonetta Geninatti Crich: 0000-0003-2998-5424

Author Contributions

The manuscript was written through contributions of all authors. All authors have given approval to the final version of the manuscript. LN. Turino and M.R. Ruggiero contributed equally.

Notes

The authors declare no competing financial interest.

■ ACKNOWLEDGMENTS

This research was funded by MIUR (PRIN 2012 code 2012SK7ASN) and by the AIRC investigator Grant IG2013 no 14565 and was also supported by Visiting Professors/Teaching Mobility programme for the academic year 2014−2015 (financed by UNITO and Fondazione CRT). This research was performed in the framework of the Consorzio Interuniversitario di Ricerca in Chimica dei Metalli dei Sistemi Biologici (CIRCMSB).

■ ABBREVIATIONS

PLGA, Poly(D, L-lactide-*co*-glicolide); PEG, poly(ethylene glycol); SCARA5, scavenger receptor class A member 5; TIM-2, T cell immunoglobulin and mucin domain-containing protein-2; TfR-1, transferrin receptors; Gd-DOTAMA, Gadolinium DOTAMA; PVA, poly(vinyl alcohol); NPs, nanoparticles; BSA, bovine serum albumin; Ferr, ferritin; CTRL, control; MRI, magnetic resonance imaging; ICP-MS, inductively coupled plasma mass spectrometry; HPLC, high pressure light chromatography; MTT, thiazoly blue tetrazolium bromide

■ REFERENCES

(1) Hare, J. I., Lammers, T., Ashford, M. B., Puri, S., Storm, G., and Barry, S. T. (2016) Challenges and strategies in anti-cancer nanomedicine development: An industry perspective. *Adv. Drug. Delivery Rev. 16*, 30135−1.

(2) Lammers, T., Rizzo, L. Y., Storm, G., and Kiessling, F. (2012) Personalized nanomedicine. *Clin. Cancer Res. 18*, 4889−4894.

(3) Pandita, D., Kumar, S., and Lather, V. (2015) Hybrid poly (lactic-co-glycolic acid) nanoparticles: design and delivery prospectives. *Drug Discovery Today 20*, 95−104.

(4) Danhier, F., Ansorena, E., Silva, J. M., Coco, R., Le Breton, A., and Préat, V. (2012) PLGA-based nanoparticles: an overview of biomedical applications. *J. Controlled Release 161*, 505−522.

(5) Davis, M. E., Chen, Z. G., and Shin, D. M. (2008) Nanoparticle therapeutics: An emerging treatment modality for cancer. *Nat. Rev. Drug Discovery 7*, 771−782.

(6) Knop, K., Hoogenboom, R., Fischer, D., and Schubert, U. S. (2010) Poly(ethylene glycol) in drug delivery: Pros and cons as well as potential alternatives. *Angew. Chem., Int. Ed. 49*, 6288−6308.

(7) Esfandyari-Manesh, M., Mostafavi, S. H., Majidi, R. F., Koopaei, M. N., Ravari, N. S., Amini, M., Darvishi, B., Ostad, S. N., Atyabi, F., and Dinarvand, R. (2015) Improved anticancer delivery of paclitaxel by albumin surface modification of PLGA Nanoparticles. *Daru, J. Pharm. Sci. 23* (28), 1−8.

(8) Darvishi, B., Manoochehri, S., Esfandyari-Manesh, M., Samadi, N., Amini, M., Atyabi, F., and Dinarvand, R. (2015) Enhanced Cellular Cytotoxicity and Antibacterial Activity of 18-β-Glycyrrhetinic Acid by Albumin conjugated PLGA Nanoparticles. *Drug Res. (Stuttgart, Ger.) 65*, 617−623.

(9) Manoochehri, S., Darvishi, B., Kamalinia, G., Amini, M., Fallah, M., Ostad, S. N., Atyabi, F., and Dinarvand, R. (2013) Surface modification of PLGA nanoparticles via human serum albumin conjugation for controlled delivery of docetaxel. *Daru, J. Pharm. Sci. 21* (58), 1−10.

(10) Finazzi, D., and Arosio, P. (2014) Biology of ferritin in mammals: an update on iron storage, oxidative damage and neurodegeneration. *Arch. Toxicol. 88*, 1787−1802.

(11) Fisher, J., Devraj, K., Ingram, J., Slagle-Webb, B., Madhankumar, A. B., Liu, X., Klinger, M., Simpson, I. A., and Connor, J. R. (2007) Ferritin: a novel mechanism for delivery of iron to the brain and other organs. *Am. J. Physiol. Cell Physiol. 293*, 641−649.

(12) Mendes-Jorge, L., Ramos, D., Valença, A., López-Luppo, M., Pires, V. M., Catita, J., Nacher, V., Navarro, M., Carretero, A., Rodriguez-Baeza, A., et al. (2014) L-ferritin binding to scara5: a new iron traffic pathway potentially implicated in retinopathy. *PLoS One*, DOI: 10.1371/journal.pone.0106974.

(13) Li, J. Y., Paragas, N., Ned, R. M., Qiu, A., Viltard, M., Leete, T., Drexler, I. R., Chen, X., Sanna-Cherchi, S., Mohammed, F., et al. (2009) Scara5 is a ferritin receptor mediating non-transferrin iron delivery. *Dev. Cell 16*, 35−46.

(14) Geninatti Crich, S., Cutrin, J. C., Lanzardo, S., Conti, L., Kálmán, F. K., Szabó, I., Lago, N. R., Iolascon, A., and Aime, S. (2012) Mn-loaded apoferritin: a highly sensitive MRI imaging probe for the detection and characterization of hepatocarcinoma lesions in a transgenic mouse model. *Contrast Media Mol. Imaging 7*, 281−288.

(15) Han, J., Seaman, W. E., Di, X., Wang, W., Willingham, M., Torti, F. M., and Torti, S. V. (2011) Iron uptake mediated by binding of H-ferritin to the TIM-2 receptor in mouse cells. *PLoS One*, DOI: 10.1371/journal.pone.0023800.

(16) Li, L., Fang, C. J., Ryan, J. C., Niemi, E. C., Lebrón, J. A., Björkman, P. J., Arase, H., Torti, F. M., Torti, S. V., Nakamura, M. C., et al. (2010) Binding and uptake of H-ferritin are mediated by human transferrin receptor-1. *Proc. Natl. Acad. Sci. U. S. A. 107*, 3505−3510.

(17) Sakamoto, S., Kawabata, H., Masuda, T., Uchiyama, T., Mizumoto, C., Ohmori, K., Koeffler, H. P., Kadowaki, N., and Takaori-Kondo, A. (2015) H-Ferritin Is Preferentially Incorporated by Human Erythroid Cells through Transferrin Receptor 1 in a Threshold-Dependent Manner. *PLoS One*, DOI: 10.1371/journal.-pone.0139915.
(18) Richardson, D. R., and Ponka, P. (1997) The molecular mechanisms of the metabolism and transport of iron in nor-mal and neoplastic cells. *Biochim. Biophys. Acta, Rev. Biomembr. 1331*, 1−40.
(19) Lui, G. Y., Kovacevic, Z., Richardson, V., Merlot, A. M., Kalinowski, D. S., and Richardson, D. R. (2015) Targeting cancer by binding iron: Dissecting cellular signaling pathways. *Oncotarget 6*, 18748−18779.
(20) Wang, W., Knovich, M. A., Coffman, L. G., Torti, F. M., and Torti, S. V. (2010) Serum ferritin: Past, present and future. *Biochim. Biophys. Acta, Gen. Subj. 1800*, 760−769.
(21) Alkhateeb, A. A., and Connor, J. R. (2013) The significance of ferritin in cancer: anti-oxidation, inflammation and tumorigenesis. *Biochim. Biophys. Acta, Rev. Cancer 1836*, 245−254.
(22) Chekhun, S. V., Lukyanova, N. Y., Shvets, Y. V., Burlaka, A. P., and Buchynska, L. G. (2014) Significance of ferritin expression in formation of malignamt phenotype of human breast cancer cells. *Exp. Oncol. 36*, 179−183.
(23) Shpyleva, S. I., Tryndyak, V. P., Kovalchuk, O., Starlard-Davenport, A., Chekhun, V. F., Beland, F. A., and Pogribny, I. P. (2011) Role of ferritin alterations in human breast cancer cells. *Breast Cancer Res. Treat. 126*, 63−71.
(24) Jutz, G., van Rijn, P., Santos Miranda, B., and Böker, A. (2015) Ferritin: a versatile building block for bionanotechnology. *Chem. Rev. 115*, 1653−1701.
(25) Ghisaidoobe, A. B., and Chung, S. J. (2015) Functionalized protein nanocages as a platform of targeted therapy and immunodetection. *Nanomedicine (London, U. K.) 10*, 3579−3595.
(26) Truffi, M., Fiandra, L., Sorrentino, L., Monieri, M., Corsi, F., and Mazzucchelli, S. (2016) Ferritin nanocages: A biological platform for drug delivery, imaging and theranostics in cancer. *Pharmacol. Res. 107*, 57−65.
(27) Kálmán, F. K., Geninatti Crich, S., and Aime, S. (2010) Reduction/dissolution of a beta-MnOOH nanophase in the ferritin cavity to yield a highly sensitive, biologically compatible magnetic resonance imaging agent. *Angew. Chem., Int. Ed. 49*, 612−5.
(28) Geninatti Crich, S., Cadenazzi, M., Lanzardo, S., Conti, L., Ruiu, R., Alberti, D., Cavallo, F., Cutrin, J. C., and Aime, S. (2015) Targeting ferritin receptors for the selective delivery of imaging and therapeutic agents to breast cancer cells. *Nanoscale 7*, 6527−6533.
(29) Fonseca, C., Simões, S., and Gaspar, R. J. (2002) Paclitaxel-loaded PLGA nanoparticles: preparation, physicochemical characterization and in vitro anti-tumoral activity. *J. Controlled Release 83*, 273−286.
(30) Mariano, R. N., Alberti, D., Cutrin, J. C., Geninatti Crich, S., and Aime, S. (2014) Design of PLGA based nanoparticles for imaging guided applications. *Mol. Pharmaceutics 11*, 4100−4106.
(31) Sahoo, S. K., Panyam, J., Prabha, S., and Labhasetwar, V. (2002) Residual polyvinyl alcohol associated with poly (D,L-lactide-co-glycolide) nanoparticles affects their physical properties and cellular uptake. *J. Controlled Release 82*, 105−114.
(32) Cheng, J., Teply, B. A., Sherifi, I., Sung, J., Luther, G., Gu, F. X., Levy-Nissenbaum, E., Radovic-Moreno, A. F., Langer, R., and Farokhzad, O. C. (2007) Formulation of functionalized PLGA−PEG nanoparticles for in vivo targeted drug delivery. *Biomaterials 28*, 869−876.
(33) Tuyen Dao, T. P., Hoai Nguyen, T., To, V. V., Ho, T. H., Nguyen, T. A., and Chien Dang, M. (2014) A new formulation of curcumin using poly(lactic-co-glycolic acid)—polyethylene glycol diblock copolymer as carrier material. *Adv. Nat. Sci.: Nanosci. Nanotechnol.*, DOI: 10.1088/2043-6262/5/3/035013.
(34) Boddu, S. H. S., Vaishya, R., Jwala, J., Vadlapudi, A., Pal, D., and Mitra, A. K. (2012) Preparation and Characterization of Folate Conjugated Nanoparticles of Doxorubicin using Plga-Peg-Fol Polymer. *Med. Chem. 2*, 68−75.
(35) Gossmann, R., Fahrländer, E., Hummel, M., Mulac, D., Brockmeyer, J., and Langer, K. (2015) Adsorption of plasma proteins on uncoated PLGA nanoparticles. *Eur. J. Pharm. Biopharm. 93*, 80−7.
(36) Sempf, K., Arrey, T., Gelperina, S., Schorge, T., Meyer, B., Karas, M., and Kreuter, J. (2013) *Eur. J. Pharm. Biopharm. 85* (1), 53−60.
(37) Esposito, G., Geninatti Crich, S., and Aime, S. (2008) Efficient cellular labeling by CD44 receptor-mediated uptake of cationic liposomes functionalized with hyaluronic acid and loaded with MRI contrast agents. *ChemMedChem 3*, 1858−62.
(38) Huang, C. H., and Tsourkas, A. (2013) Gd-based macromolecules and nanoparticles as magnetic resonance contrast agents for molecular imaging. *Curr. Top. Med. Chem. 13*, 411−421.
(39) Rowinsky, E. K., and Donehower, R. C. (1995) Paclitaxel (taxol). *N. Engl. J. Med. 332*, 1004−1014.
(40) Gelderblom, H., Verweij, J., van Zomeren, D. M., Buijs, D., Ouwens, L., Nooter, K., Stoter, G., and Sparreboom, A. (2002) Influence of Cremophor El on the bioavailability of intraperitoneal paclitaxel. *Clin. Cancer Res. 8*, 1237−1241.
(41) Weiss, R. B., Donehower, R. C., Wiernik, P. H., Ohnuma, T., Gralla, R. J., Trump, D. L., Baker, J. R., Jr., Van Echo, D. A., Von Hoff, D. D., and Leyland-Jones, B. (1990) Hypersensitivity reactions from taxol. *J. Clin. Oncol. 8*, 1263−1268.
(42) Averineni, R. K., Shavi, G. V., Gurram, A. K., Deshpande, P. V., Arumugam, K., Maliyakkal, N., Meka, S. R., and Nayanabhirama, U. (2012) PLGA 50:50 nanoparticles of paclitaxel: Development, in vitro anti-tumor activity in BT-549 cells and in vivo evaluation. *Bull. Mater. Sci. 35*, 319−326.
(43) Chittasupho, C., Lirdprapamongkol, K., Kewsuwan, P., and Sarisuta, N. (2014) Targeted delivery of doxorubicin to A549 lung cancer cells by CXCR4 antagonist conjugated PLGA nanoparticles. *Eur. J. Pharm. Biopharm. 88*, 529−538.
(44) Shah, N., Chaudhari, K., Dantuluri, P., Murthy, R. S., and Das, S. (2009) Paclitaxel-loaded PLGA nanoparticles surface modified with transferrin and Pluronic((R))P85, an in vitro cell line and in vivo biodistribution studies on rat model. *J. Drug Targeting 17*, 533−542.
(45) Yu, K., Zhao, J., Zhang, Z., Gao, Y., Zhou, Y., Teng, L., and Li, Y. (2016) Enhanced delivery of Paclitaxel using electrostatically-conjugated Herceptin-bearing PEI/PLGA nanoparticles against HER-positive breast cancer cells. *Int. J. Pharm. 497*, 78−87.
(46) Danhier, F., Lecouturier, N., Vroman, B., Jèrôme, C., Marchand-Brynaert, J., Feron, O., and Préat, V. (2009) Paclitaxel-loaded PEGylated PLGA-based nanoparticles: in vitro and in vivo evaluation. *J. Controlled Release 133*, 11−17.
(47) Anelli, P. L., Lattuada, L., Lorusso, V., Schneider, M., Tournier, H., and Uggeri, F. (2001) Mixed micelles containing lipophilic gadolinium complexes as MRA contrast agents. *Magma 12*, 114−20.
(48) Sahoo, S. K., Ma, W., and Labhasetwar, V. (2004) Efficacy of transferrin-conjugated paclitaxel-loaded nanoparticles in a murine model of prostate cancer. *Int. J. Cancer 112*, 335−340.

DOI: 10.1021/acs.bioconjchem.7b00096
Bioconjugate Chem. 2017, 28, 1283−1290